Durability and transport properties of SCC incorporating dredged sediments

Amine El Mahdi Safhi, Patrice Rivard, Ammar Yahia, Kamal Henri Khayat, Nor-Edine Abriak

Durability and transport properties of SCC incorporating dredged sediments

Amine el Mahdi Safhi [1, 2, 3 *], **Patrice Rivard** [3], **Ammar Yahia** [3], **Kamal Henri Khayat** [4], **Nor-Edine Abriak** [2]

[1] Mohammed VI Polytechnic University, EMEC Program, Ben Guerir, Morocco

[2] Université de Lille, Institut Mines-Télécom Lille Douai, ULR 4515 - LGCgE, Douai, France

[3] Université de Sherbrooke, Civil and Building Engineering Department, Sherbrooke, Canada

[4] Missouri S&T, Center for Infrastructure Engineering Studies, Rolla, MO, USA

ABSTRACT

The use of sediments as supplementary cementitious material is increasing, but very limited information on their effect on durability are available. The aim of this study is to evaluate the durability and transport properties of self-consolidating concrete (SCC) incorporating treated marine sediments (TMS) dredged from Dunkirk harbor. Three SCC mixtures made with 0% (SCC-R), 10% (SCC-1), and 20% (SCC-2) sediments as partial substitution of cement weight were investigated. The mixture proportions were optimized to provide adequate self-consolidating characteristics, including high filling and passing abilities, as well as adequate stability. The optimized SCC mixtures exhibited comparable hardened and microstructural properties at 91 days of age, including compressive strength of 66 ± 1 MPa, splitting tensile strength of 6 ± 0.3 MPa, and total porosity of 9 ± 0.4 %. The obtained test results revealed that the incorporation of TMS reduced the critical pore volume (< 20 nm) due to their pozzolanic reaction and filling ability. Despite this reduction, increasing TMS content increased permeability and diffusion (e.g., carbonation). Indeed, SCC-1 and SCC-2 showed higher sorptivity of 7.5% and 19.8%, respectively, than that of SCC-R

* Corresponding author: Amine el Mahdi Safhi

Email: amineelmahdi.safhi@um6p.ma

Current address: Mohammed VI Polytechnic University, EMEC Program, Ben Guerir, Maroc

(2.81 E^{-3} $mm^3/mm^2.s^{½}$). However, SCC-1 showed comparable durability performance to the reference mixture, including chloride penetrability, electrical resistivity, drying shrinkage, external sulfate attack, and alkali-silica. Meanwhile, the use of 20% TMS negatively influenced the chloride penetrability, external sulfate attack, and carbonation velocity. This substitution rate can be considered without mitigating durability of reinforced concrete in moderate exposure conditions.

Keywords: Blended cement; Dredged sediment; Durability; Self-consolidating concrete; Supplementary cementitious materials; Transport properties.

1. INTRODUCTION

In compliance with the EN 206-1 specifications [1], concrete performance encompasses mechanical properties and durability. The reported "Performance-based Approach" is based on testing relevant durability indicators given predefined exposure classes, such as corrosion, chemical attacks, and/or physical degradation [2]. Concrete durability is greatly related to its transport properties, including permeability, sorptivity, and diffusion. These properties are governed by the pore structure of the matrix and their connectivity. Durable concrete requires lower porosity and permeability to limit penetration of aggressive ions due to diffusion and capillary absorption [3] depending on the targeted exposure conditions. Durability improvement can be achieved by using supplementary cementitious materials (SCMs). Indeed, the pozzolanic activity of SCMs consume calcium-hydroxide (CH) produced during cement hydration to form additional calcium-silicate-hydrate (C-S-H). This can lead to a dense microstructure, reduces the permeability of the hydrated cement, thus lowering ingress of chlorides (reinforcement corrosion) [4] and carbon dioxide (concrete carbonation) [5].

Partial replacement of cement with SCMs is an efficient way to reduce the demand for natural resources and decrease the CO_2 footprint. SCMs contain a large amount of amorphous silica and alumina, which can react with calcium hydroxide in hydrating cement to form additional hydration products. Industrial by-products, including fly ash, ground blast furnace slag, and silica fume have

been used as SCMs for many decades. In addition, various sub-products such as ceramic waste powder [6], waste perlite powder [7], raw diatomite [8], natural zeolite [9], as well as nanomaterials, i.e. silicon dioxide (SiO_2), titanium oxide (TiO_2), aluminum oxide (Al_2O_3), calcium carbonate ($CaCO_3$), zirconium oxide (ZrO_2), ferric oxide (Fe_2O_3), clay, and carbon nanotube [10,11] have been used as SCMs. The use of SCMs is essential to increase the volume of paste and enhance workability of self-consolidating concrete (SCC). However, the limited availability of natural resources opens the way for searching viable source for SCM. Dredged sediments appeared to be good alternative SCMs as they are available in huge quantities exceeding one-billion-meter cube per year all over the world [12–14].

The pozzolanic potential of dredged sediments has been reported in literature [14–16]. However, very limited studies have been carried out to evaluate their effect as SCMs on properties and durability performances of SCC [17–19]. Rozas et al. [17] provided a guideline to assess the performance of recycled dredged sediments from Spanish Mediterranean Harbor, which were used as filler. Only one mixture was tested using 450 kg/m^3 of cement, 100 kg/m^3 of dredged sediments, and a w/c ratio of 0.45. The investigated concrete exhibited compressive strength of 44 MPa, total porosity average of 9.2%, electrical resistivity of 49 kΩ.cm, chloride diffusion coefficient (Ds) of 1.12 E^{-8} cm²/s, and capillary absorption of 1.44 E^{-3} kg/m².min$^{1/2}$ after 28 days of age. In accordance with the durability indicators described in “Concrete design for a given structure service life” in the Spanish Code on Structural Concrete (EHE-08), the authors claimed that sediments can be used as fillers in SCC, although tests have been conducted on only one mixture. Rozière et al. [18] used dredged sediments as total replacement of limestone filler for SCC production. Sediments were collected from the Dampremy - Charleroi region in Belgium and treated using the Novosol® process (phosphatation and calcination). In the case of a constant w/c ratio of 0.57, the sediments-based SCC showed approximately 8% drop in slump flow, higher yield stress and plastic viscosity, as well as workability loss. However, comparable compressive strength and density were found at different ages. Nanoindentation measurements showed that the elastic modulus of hydrated cement pastes in

74 the sediment-based SCC was 27 GPa (16% higher than the reference mixture). Bouhamou et al.
75 [19] investigated the influence of 10%, 15%, and 20% replacements of cement by calcined dam
76 mud sediments on the shrinkage of SCC. The sediments were dredged from the dam of Fergoug in
77 Algeria and treated at a temperature of 750 °C. The authors reported that the use of calcined mud
78 resulted in viscous and less workable SCC mixtures. Also, the sediments showed a negative effect
79 on strength, but the use of 10% sediments did not significantly affect the compressive strength (less
80 than 10% variation) compared to the control mixture. Moreover, lower autogenous and drying
81 shrinkage values were observed. Indeed, SCC containing 20% of sediments developed a total
82 drying shrinkage of 150 μm/m after 90 days of exposure, which is 23% less than the control
83 mixture. This paper is part of a wide investigation on valorizing sediments from Dunkirk Port as
84 SCM in SCC mixtures.

85 2. RESEARCH SIGNIFICANCE

86 Previous investigations on pastes and mortars [20,21] revealed that dredged marine sediments
87 did not show negative effect on fresh properties when the water demand of sediment is taken into
88 account. Using a multi-objective optimization for workability properties and compressive strength
89 development at different ages, an optimal substitution content of 7% to 35% were reported in the
90 case of binder content ranging between 380 and 600 kg/m^3 and water-to-cementitious materials
91 (*w/cm*) of 0.32 and 0.34. Based on these findings, a scale-up study of these sediments has been
92 conducted to evaluate their effect of durability of SCC [22]. The investigated SCC mixtures were
93 proportioned with total binder content of 450 kg/m^3, two different sediment's contents of 10% and
94 20%.

95 The investigated SCC mixtures exhibited adequate self-consolidation characteristics with high
96 filling ability, high passing ability, and high stability resistance. Furthermore, the investigated SCC
97 mixtures showed similar compressive strength of 66 ± 1 MPa and a total porosity of 9% at 91 days
98 of age. This was attributed to the pozzolanic reaction of the sediments that contributed to refining
99 microstructure of the interfacial transition zone (ITZ). Nevertheless, durability study of those SCC

mixtures was not established. This paper investigated the durability indicators and transport properties, including capillary absorption, sorptivity, chloride penetrability, electrical resistivity, drying shrinkage, external sulfate attack, alkali silica reaction, and accelerated carbonation of the investigated SCC mixture containing dredged marine sediments provides useful information on the use of TMS in SCC production, which goes along with the 3R concept, Reduce, Recycle, and Reuse.

3. MATERIALS, MIXTURE PROPORTIONS, AND METHODOLOGY

3.1. Constituent materials

The investigated mixtures were proportioned using a ternary binder complying with the ASTM C150 specifications [23]. The binder is composed of 70% General Use (GU) cement, 25% Class F fly ash, and 5% of silica fume. It has a specific density of 2890 kg/m^3 and a BET surface area of 2535 m^2/kg. Two crushed coarse aggregates CA_1 (10/20 mm) and CA_2 (5/10 mm) were used. The CA_1 and CA_2 have specific densities of 2.76 and 2.72 g/cm^3, absorption rates of 0.48% and 0.41%, and bulk densities of 1465 and 1444 kg/m^3, respectively. A siliceous river sand with a specific density of 2.66 g/cm^3, an absorption rate of 1.09%, and a bulk density of 1785 kg/m^3 was used.

The sediments were collected from the Dunkirk Harbor in France, dried in an oven at 60 °C, and subsequently ground and sieved on 2-mm sieve. The sediments were heated at 800 °C for one hour to eliminate water-content, organic matter, and chemically activate the raw sediments. After the calcination process, the obtained product was sieved to meet a d_{50} less than 45 μm comparable to that of cement. The density of the sediments increased from 2467 to 2704 kg/m^3 after one hour of thermal treatment. The treated marine sediment (TMS) has a BET surface area of 3143 m^2/kg, which is 24% higher than that of cement. Its chemical composition determined using XRF spectrometry analysis revealed that it can be considered as pozzolan according to the ASTM C618 specifications [24]. It is composed of 72% silica, 9.7% calcium oxide, 5.3% ferrite oxide, and 3.8%

aluminum oxide. In addition, its SO_3 content is below 0.1%, which is considerably below the maximum limit of 4%. The chemical composition of the sediments is similar to that of ground glass powder reported in different studies [25–34], as shown in Fig. 1.

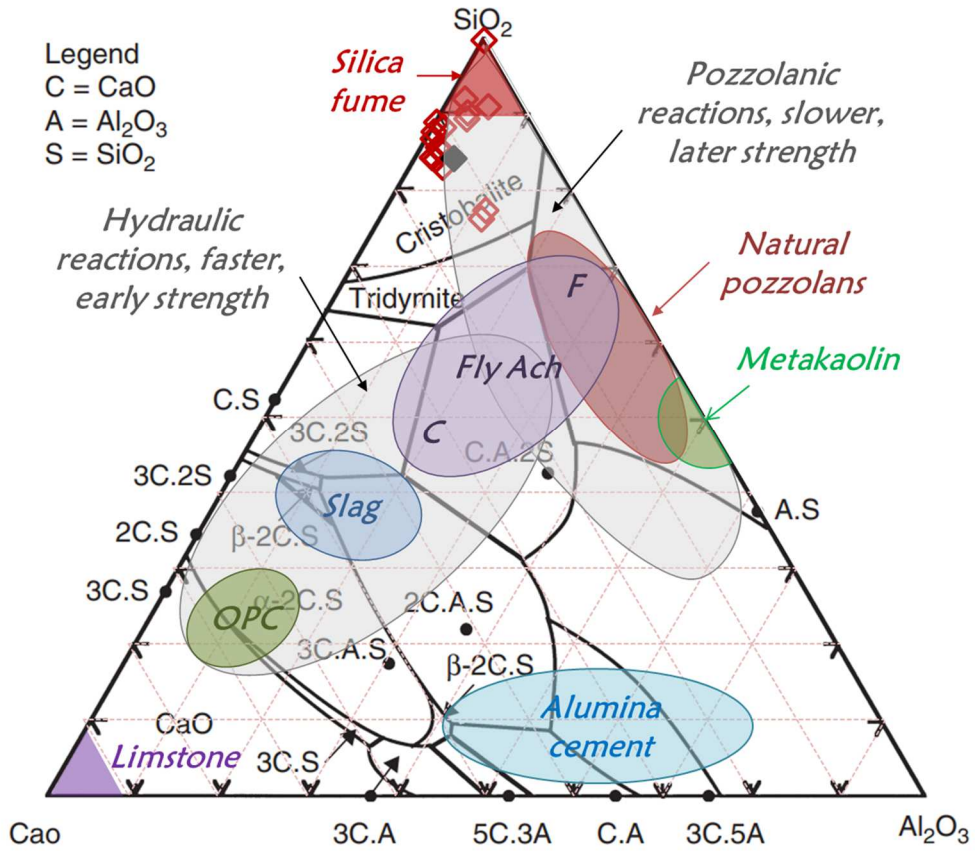

Fig. 1: Composition of TMS (black), composition of ground glass powder cf. [25–34], superimposed on mainly used SCMs, adapted from [35,36]

The particle-size distribution was determined using a laser diffraction Coulter complied with ISO 13320 specifications. The median particle-size of the sediment is 17 µm compared to 13 µm for cement. Shao et al. [28] reported that 30% cement replacement by glass particles (73% silica) of 30 µm size resulted in 14% and 33% higher compressive strength than concrete made with powder of 75 µm and 150 µm, respectively. The detailed characterization of the raw and treated sediments were reported by Safhi et al. [22].

3.2. Mixtures proportioning and mixing sequence

In addition to the control SCC mixture (SCC-R), two SCC mixtures incorporating 10% (SCC-1) and 20% (SCC-2) of TMS were prepared (Table 1). All of the investigated mixtures were proportioned with a *w/c* of 0.40 plus an additional water corresponding to 0.35 of the mass of TMS was added to secure adequate workability; this water content was determined using the method proposed by Sedran et al. [37] for water demand. The sand, CA_1, and CA_2 contents were 893, 147, and 578 kg/m^3, respectively. These proportions were optimized in a previous study to achieve well-graded skeleton and maximum packing density [22]. A commercial high-range water-reducer (HRWRA) was incorporated at a dosage of 1200 ml/100 kg of cementitious materials to achieve a targeted slump flow (S_{flow}) of 680 ± 20 mm. All the investigated mixtures were prepared in batches of 60 l using a rotating drum mixer. The mixing sequence consists of homogenizing sand for 30 s, followed by adding coarse aggregate and mixing for 60 s. One third of the water was then added, and the material was mixed for 30 s. The cementitious materials were added and mixed for 30 s before introducing HRWRA diluted with one third of mixing water. The concrete was then mixed for an additional 120 s before introducing the last portion of mixing water. The concrete was mixed for 60 s and left to rest for 2 min, after which the mixing was resumed for another 3 min.

Table 1: Mixture proportions of the investigated SCC mixtures, content in kg/m^3

Mixture	***Cement***	***TMS***	***CA_1***	***CA_2***	***Sand***	***Water***		
						Base w/c = 0.4	***Additional water for TMS (w/TMS) = 0.35***	***Total***
SCC-R	450	0	147	578	893	180	0	180
SCC-1	405	45				162	15.8	178
SCC-2	360	90				144	21.5	176

3.3. Tests methods

After the mixing process, fresh properties were measured, and various samples were prepared to determine the hardened properties. Each sample was cast in one layer without any vibration.

157 Immediately after casting, specimens were properly covered to avoid water evaporation and left
158 undisturbed at room temperature of 23 ± 2°C. After 24 ± 4 h, the specimens were demolded and
159 transferred to a curing chamber at 95% relative humidity (RH) and controlled temperature of 23 ±
160 2°C until the age of testing. Table 2 summarizes the tests conducted on the mixtures. For each test,
161 measurements were made on three different samples.

162 *Table 2: Test methods of the investigated mixtures*

Properties		***Test method***	***Samples***	***Testing periods***
Fresh properties				
Filling ability	S_{flow} *(mm)*	ASTM C 1611 [38]	-	Fresh
	T_{50} *(s)*		-	Fresh
	V_{funnel} *time (s)*	EN 12350-9	-	Fresh
Passing ability	J_{Ring} *flow (mm)*	ASTM C 1621 [39]	-	Fresh
	L-box flow	EN 12350-10	-	Fresh
Stability	*Sieve segregation (%)*	EN 12350-11	-	Fresh
Air content (%)		ASTM C 231 [40]	-	Fresh
Unit weight (kg/m^3)		ASTM C 138	-	Fresh
Hardened mechanical properties				
Compressive strength		ASTM C 39 [41]	100 Ø 200 mm	3, 28, 56, and 91 days
Split tensile strength		ASTM C 496 [42]		
Durability properties				
Mercury porosimetry		NF P18- 459	Inner fragments	91 days
Electrical resistivity		ASTM C 1760 [43]	100 Ø 200 mm	3, 28, 56, and 91 days
Rapid chloride ion penetrability		ASTM C 1202 [44]	100 Ø 50 mm	91 days
Absorption and sorptivity		ASTM C 1582 [45]	100 Ø 50 mm	-
Drying shrinkage		ASTM C 157 [46]	25 mm^2 x 285 mm	-
External sulfate attack		ASTM C 1012 [47]	25 mm^2 x 285 mm	-
Alkali silica reaction (ASR)		ASTM C 1260 [48]	25 mm^2 x 285 mm	-
Accelerated carbonation		-	100 mm^2 x 50 mm	3, 28, 56, and 91 days

The accelerated carbonation tests were conducted using a special chamber in which 4.0% of carbon dioxide was introduced at controlled relative humidity of 55% ± 5% and temperature of 20 ± 2°C. For each SCC mixture, three 100 mm^2 by 400 mm prisms were tested. The prisms were prepared and wet cured for 28 days. They were then left to dry for 14 days at 50% relative humidity before carbonation testing. The carbonation depths (x_c) were evaluated by spraying 1% phenolphthalein alcohol solution on a specimen of 100 mm^2 by 50 mm cut at different ages of the test. The non-carbonated region is identified by purple color due to high alkalinity. The x_c was determined by taking the average depth of colorless regions.

4. RESULTS AND DISCUSSIONS

4.1. Workability

The fresh properties of the investigated SCC mixtures are summarized in Table 1. As can be observed, the investigated mixtures achieved a S_{flow} of 690 ± 5 mm, which corresponds to SCC Class 2 (SF2) in accordance with EFNARC standard [49]. Also, all the investigated mixtures exhibited a comparable T_{50} value of approximately 2 sec and good passing ability reflected by difference between S_{flow} and J_{Ring} flow values (i.e., S_{flow} - J_{Ring}) less than 50 mm [50]. The mixtures achieved a V_{funnel} flow time ranging between 6 and 8 s, and a blocking index H_2/H_1 between 0.85 and 0.98 in the L-box test [51]. The investigated mixtures belong to passing ability class "PA1", except for the SCC-2. On the other hand, the segregation index of the investigated mixtures was less than 10%. It is worth mentioning that during the test, no sign of bleeding was noticed at the outer edge of the spread. This indicates that all the developed SCCs an adequate segregation and bleeding resistance. The findings indicate that the investigated mixtures have good passing ability and stability.

Table 3: Fresh properties of the studied mixtures

Properties		***SCC-R***	***SCC-1***	***SCC-2***
Filling	*S_{flow} (mm)*	695	690	685

ability	T_{50} *(s)*	2.00	2.03	2.06
	V_{funnel} *time (s)*	8.10	7.41	6.66
Passing ability	J_{Ring} *flow (mm)*	655	660	665
	L-box flow	0.98	0.94	0.85
Stability	*Sieve segregation (%)*	6.6	8.5	6.2
Air content (%)		3.9	2.2	1.4
Specific gravity (kg/m^3)		2310	2365	2380

4.2. Hardened properties

The average compressive and splitting tensile strength values of the SCCs mixtures are presented in Fig. 2. The investigated mixtures showed similar trend of strength development with time. The increase rate was rapid up to 28 days and then slowed down afterward. A previous study conducted on the same mixtures [22] reported the evolution of ultrasonic pulse velocity reflecting the ongoing hydration reactions toward the formation of a denser and interlocked microstructure. The investigated mixtures reached a velocity of 4900 m/s and exhibited similar compressive strength of 66 ± 1 MPa at 91 days of age. The maximum strength was observed with SCC-1 containing 10% TMS, regardless of the age. The oxides derived from TMS contribute to the pozzolanic reactivity and produce additional calcium silicate hydrate (C–S–H), hence leading to higher strength development [22]. The SCC-2 mixture containing 20% TMS showed a slower strength gain but reached comparable strength after 91 days of age. It is well known that the use of SCMs required longer curing time to achieve a given strength. Du and Tan [26] reported that concrete incorporating 60% of glass powder that contains 72% silica exhibited a compressive strength of 22 MPa after 7 days of age compared to 35 MPa obtained in the case of the reference mixture. However, after 365 days of age, the glass-powder concrete containing showed 12% greater compressive strength than the reference mixture.

The tensile strength of SCC-1 was comparable to that of the reference mixture. The increase of TMS content resulted in a slight decrease in splitting strength. This may be due to the low liberated quantity of lime during hydration compared to the available quantity of silica in the case of higher

substitutions of 20%. Also, the relatively higher finesse of TMS compared to that of cement can induce higher water demand for a given workability that leads to lower strength [52]. The partial replacement of cement by 20% of TMS can also result in lower C_3S phases in blended cement, hence reducing the volume of initial hydration products. After 91 days of age, the investigated SCC mixtures exhibited a comparable tensile strength of 6 ± 0.3 MPa. Sharifi et al. [25] reported similar results with the use of glass microparticles as partial replacement of cement (up to 30%, by weight). The authors reported that the mixture containing 5% of ground waste glass exhibited the highest compressive strength, regardless of the age of concrete. However, the use of substitution rates higher than 20% resulted in decreasing the compressive strength development due to the excess silica content.

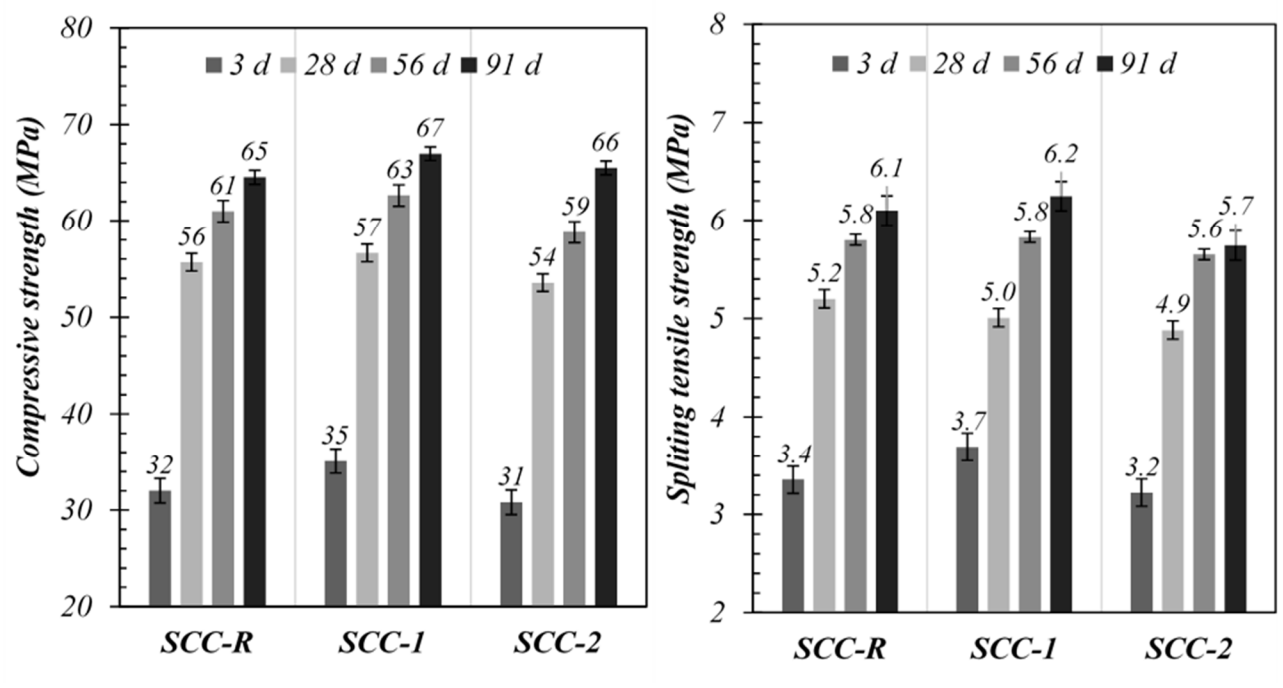

Fig. 2: Compressive and tensile splitting strengths of SCCs at different ages

4.3. Microstructure characteristics

Pore structure and porosity of cementitious materials depend mainly on the reactivity of cement, *w/cm* ratio, curing temperature and condition and SCMs which refine the pore structure [53]. The pore-size distribution of the investigated SCC mixtures is illustrated in Fig. 3. As can be observed, the mixtures exhibited an average total porosity of 9.1%. SCC-R mixture showed the

lowest porosity (8.74%), while SCC-2 exhibited the highest one (9.57%). However, the TMS mixtures exhibited more refined pores less than 20 nm compared to the reference mixture. This can be explained by the densification of the ITZ caused by additional formed C-S-H gels attributed to the high chemical activity and pozzolanic reaction of TMS. SEM observations show that SCC-1 is denser than SCC-2 mixture (Fig. 4). Refined and denser ITZ is crucial to achieve durable concrete, since it is the preferential pathway of transport properties (e.g. permeability, diffusion, etc.). In fact, the use of TMS increased the capillary porosity because of the higher effective *w/cm* ratio in the presence of TMS which required water to ensure the targeted workability [54]. Higher substitution rate of cement by finer SCMs increases the nucleation zones, hence increasing hydration kinetics. Similar findings were reported using glass powder that led to finer pores size with a comparable total porosity [26].

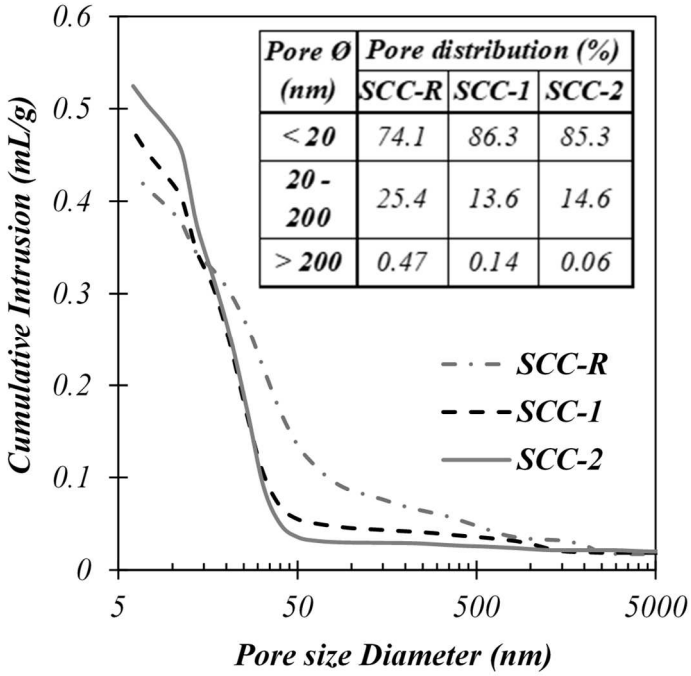

Fig. 3: Pore structure and distribution of SCC fragments at 91 days

SCC-R	SCC-1	SCC-2

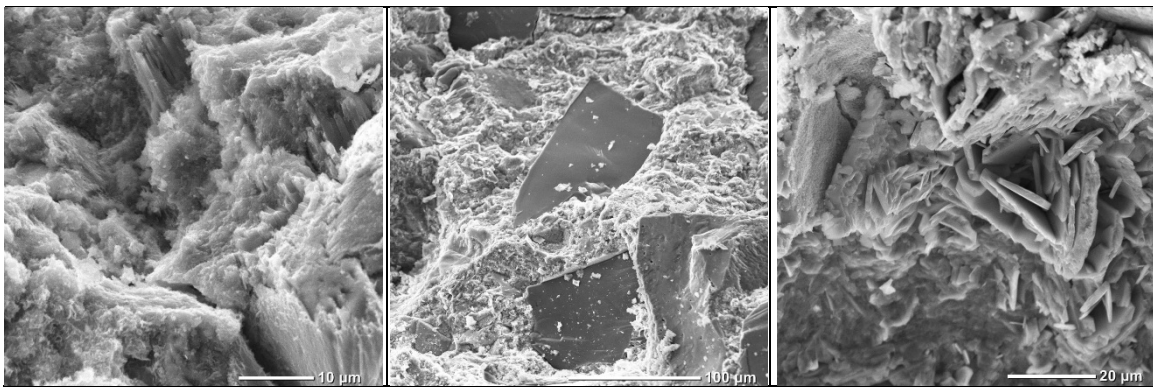

Fig. 4: SEM images of the investigated systems at 91 days

4.4. Transport Properties and Durability

4.4.1. Absorption and Sorptivity

Absorption and sorptivity are the principally transport mean of harmful agent (e.g. chloride, acid, sulfate, etc.) in concrete. The reachable pore volume represents the average value (*I*) obtained on three different samples (Fig. 5). As expected, the water absorption increased with time, regardless of the mixture type. The SCC-R and SCC-1 mixtures showed comparable initial adsorption values, while SCC-2 mixture showed relatively higher value. The presence of TMS increased the secondary absorption, which indicates a higher pores connectivity. The sorptivity represents the slope of the cumulative absorbed volume of liquid per unit inflow surface versus $t^{½}$ curve. This property was determined with accuracy of ± 5 E^{-5} $mm^3/mm^2.s^{½}$. As shown schematically in Fig. 5, the sorptivity test can be divided into two phases, a higher slope during the first 6h of testing corresponding to the initial sorptivity (S_1), which is related to the capillary suction. The lower slope corresponds to the secondary sorptivity (S_2), which is related to the filling of pores and air voids [55]. The S_1 values for the mixtures containing 10% and 20% of TMS are higher than that of SCC-R mixture by 7.5% and 19.8%, respectively. On the other hand, the S_2 values were 37% and 62% higher than that of SCC-R mixture, respectively. Nevertheless, for all the investigated mixtures, sorptivity values were less than 0.05 $mm^3/mm^2.s^{½}$, which indicates a good durability according to the Concrete Society criteria [56].

255 It is worthy to mention that a higher TMS substitution necessitates a higher *w/c*, hence resulting
256 in higher porosity and sorptivity as well as deep water penetration and higher absorption. Liu [57]
257 reported that sorptivities of SCC incorporating glass powder increased with substitution content.
258 On the other hand, Nassar and Soroushian [58] reported that concrete containing 20% of milled
259 glass showed 13% less water absorption after 56 days of age compared to the reference mixture.
260 This can be attributed to the pozzolanicity and filling effect of the glass powder. However, Matos
261 and Sousa-Coutinho [59] reported that the use of 20% of glass powder did not influenced the
262 sorptivities of concrete. This can be attributed to the fact that glass powder and cement had
263 comparable finesse.

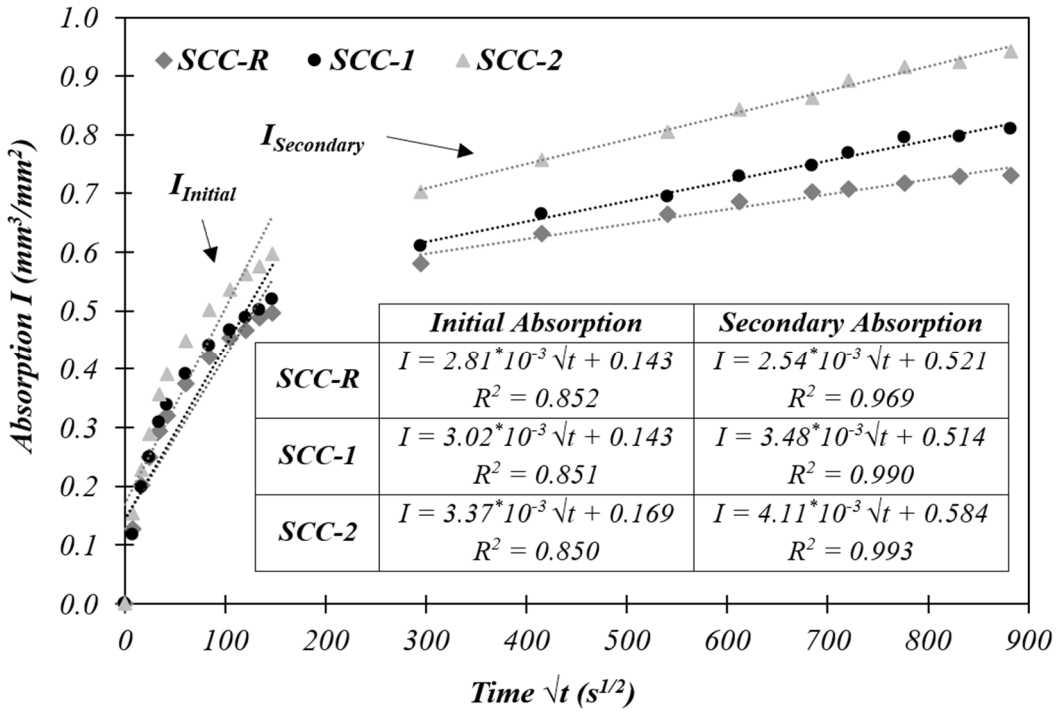

	Initial Absorption	Secondary Absorption
SCC-R	$I = 2.81^{*}10^{-3}\sqrt{t} + 0.143$, $R^2 = 0.852$	$I = 2.54^{*}10^{-3}\sqrt{t} + 0.521$, $R^2 = 0.969$
SCC-1	$I = 3.02^{*}10^{-3}\sqrt{t} + 0.143$, $R^2 = 0.851$	$I = 3.48^{*}10^{-3}\sqrt{t} + 0.514$, $R^2 = 0.990$
SCC-2	$I = 3.37^{*}10^{-3}\sqrt{t} + 0.169$, $R^2 = 0.850$	$I = 4.11^{*}10^{-3}\sqrt{t} + 0.584$, $R^2 = 0.993$

264

265 *Fig. 5: Capillarity absorption of the investigated SCC mixtures*

266 **4.4.2. Electrical resistivity and chloride penetrability**

267 As can be observed in Fig. 6, the electrical resistivity of the investigated SCC increased with
268 time, regardless of type and age of the mixture. This is probably due to the pore refinement induced
269 by the pozzolanic reaction. SCC-1 mixture showed the highest resistivity compared to control
270 mixture (+8.1% at 91 days). On the other hand, SCC-2 showed a comparable resistivity than control

mixture up to an age of 28 days but decreased by 8.0% and 9.8% after 56 and 91 days of age, respectively. In general, the use of 10% TMS resulted in higher volume of micropores less than 20 nm, hence resulting in denser matrix and higher electrical resistivity. However, the use of 20% TMS resulted in higher porosity and less compact matrix, thus inducing lower electrical resistivity. Electrical resistivity is also affected by the pore solutions, principally the presence of Ca^{2+} and OH^- ions. The increase in TMS substitution content lowered the concentration of these ions, hence lowering the electrical conductivity [26]. This is consistent with reported literature on the use of pozzolanic materials to improve resistivity despite their low contribution to strength development of concrete [60]. Overall, the electrical resistivity of the investigated mixtures was higher than 20 kΩ.cm, which indicates a low risk of corrosion [61].

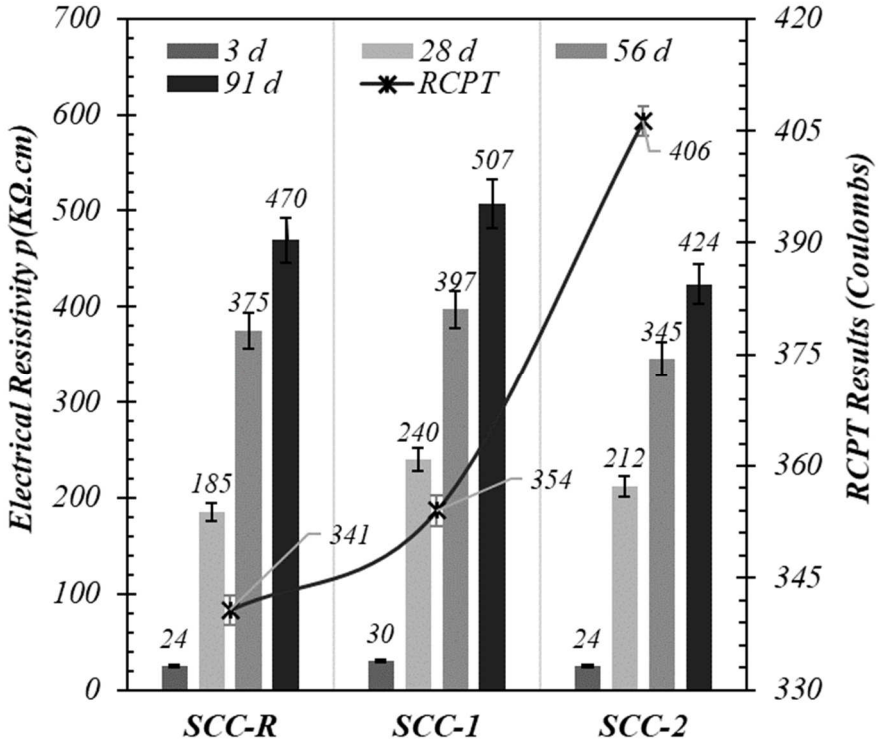

Fig. 6: Electrical resistivity and chloride penetrability of SCC mixtures

Chloride resistance is a key property that can affect the lifetime of steel in reinforced structure, especially in marine conditions. Capillary suction, diffusion, penetrability, migration, or combinations of these transport mechanisms can be used to assess chloride ions ingress into concrete. Based on the Fick's 2nd law, the apparent diffusion coefficient is usually used for

measuring chloride penetrability. In this study, the "Rapid chloride penetrability test" (RCPT) was conducted on SCC samples at 91 days of age to determine the apparent diffusion coefficient. The results of the RCPT showed a reasonable correlation with the results of the diffusion coefficients; however, a significant spread of data was obtained considering the log-log plot (Fig. 7). As reported by Thomas [62], the relation between RCPT and diffusion coefficient is primarily governed by the pore structure (volume, size, connectivity, and tortuosity of the pores), and to a lesser degree by the composition of cement hydrates and pore solution.

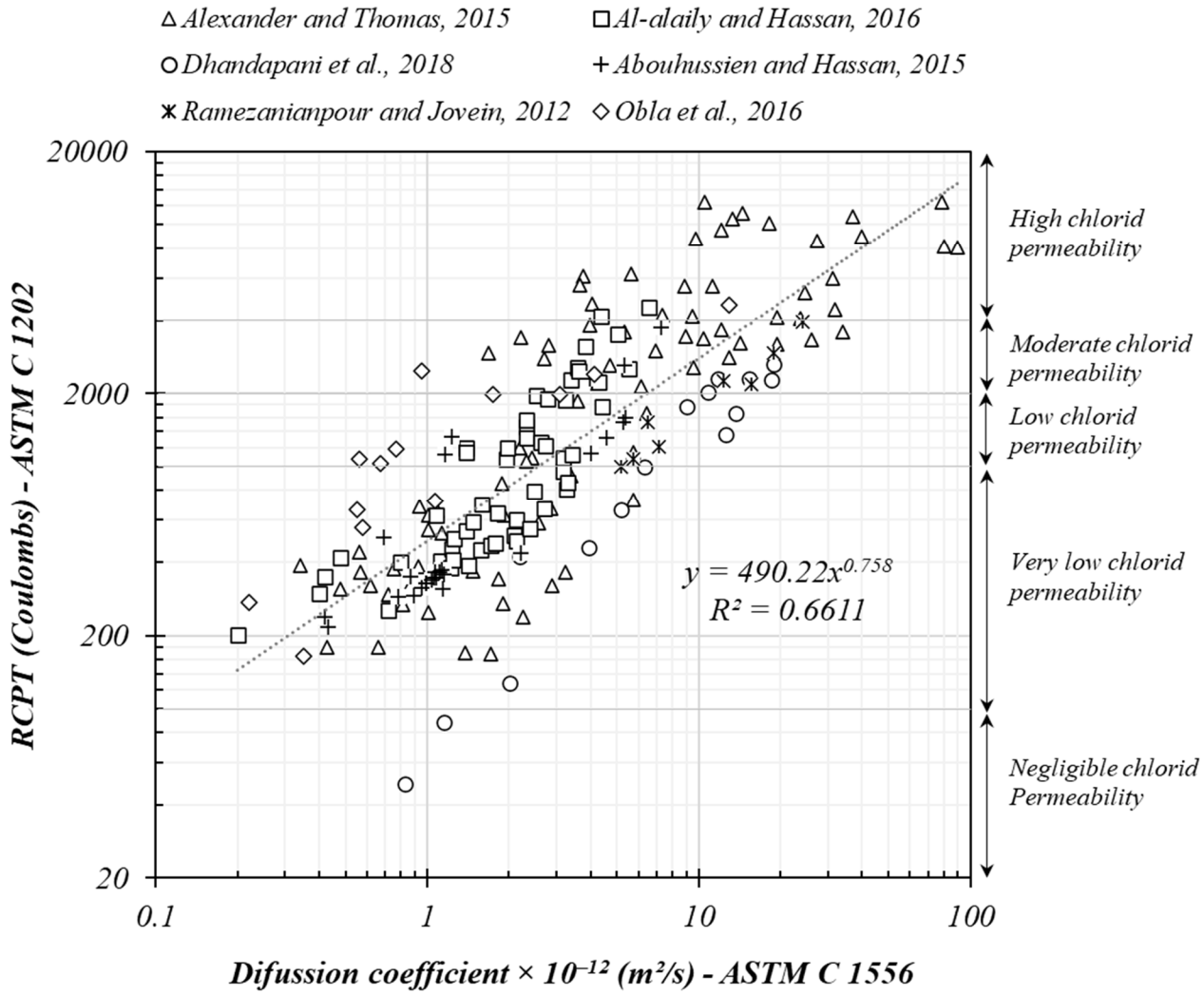

Fig. 7: Correlation between 201 test data of RCPT and diffusion coefficient results (data of 28 days were chosen) – cf. [63–68]

As can be observed in Fig. 6, the test results revealed that the investigated mixtures achieved RCPT values lower than 1000 Coulomb, which indicates a very low chloride permeability (ASTM

C1202). SCC-1 and SCC-2 mixtures showed, however, 4% and 19% higher RCPT values, respectively, than control mixture (341 Coulombs). This tendency is similar to that observed with sorptivity values. Nassar and Soroushian [58] reported that the use of well ground glass powder (d_{50} equal 13 µm) reduced chloride penetrability due to the pozzolanic reaction that refine the porosity of the matrix. The TMS used in this study is a fine powder having a d_{50} of 17 µm, hence improving the microstructure and transport properties.

4.4.3. Unrestrained drying shrinkage

Unrestrained shrinkage testing was carried out to determine the free volumetric change of concrete according to the ASTM C157 specifications [46]. As can be observed in Fig. 8, the investigated mixtures achieved comparable length change values at 7 days of exposure. However, drying shrinking developed quickly after 7 days of exposure, and stabilized after 21 days. SCC-R control mixture exhibited higher shrinkage of 8% and 5% after 49 days of exposure than SCC-1 and SCC-2 mixtures, respectively. The microstructure analysis is consistent with the shrinkage results reported in this study, where SCC-R showed the lowest volume of micro-pores and the highest volume of meso-pores. The test results revealed that the mass loss increased with TMS content compared to control mixture. Indeed, SCC-1 and SCC-2 mixtures showed 5% and 12% higher mass loss, respectively, than control mixture. These results are similar to those reported on the effect of red mud on drying shrinkage of concrete [5]. This reduction was attributed to the porosity of red mud and its ability to absorb a large volume of free water and thereafter released it, hence contribute to reducing drying shrinkage through internal curing process.

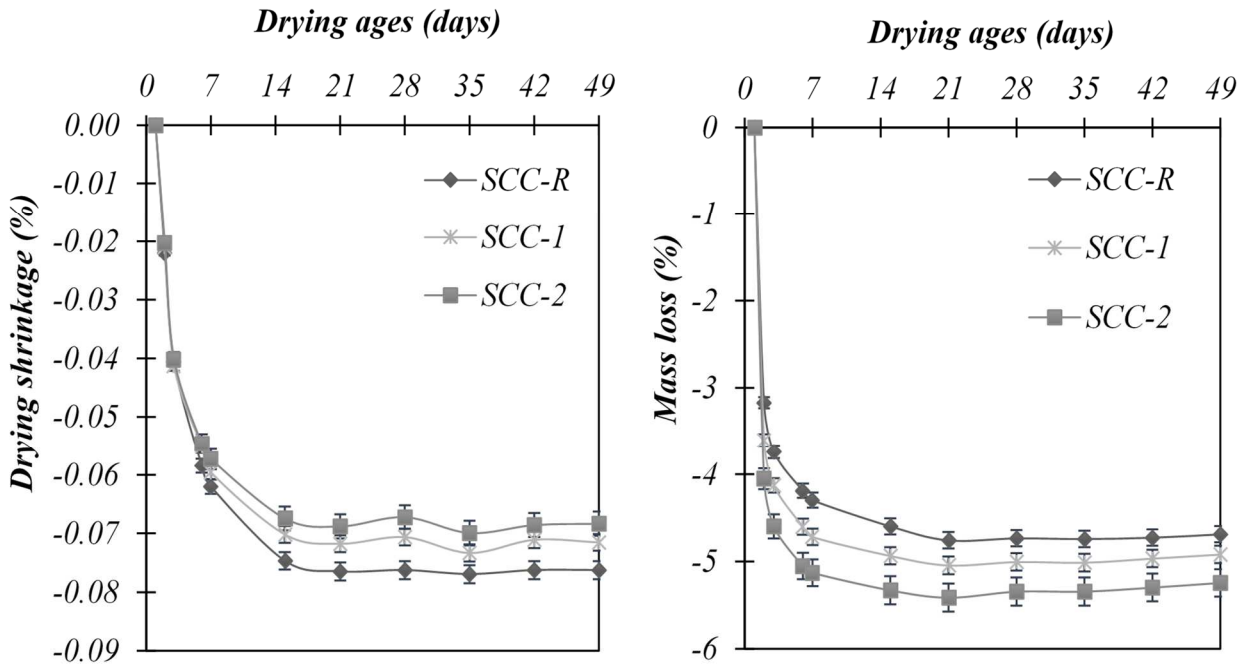

Fig. 8: Drying shrinking: length change (left) and mass loss (right)

Bouhamou et al. [19] investigated the influence of dredging sediments used as SCM on shrinkage of SCC. The authors reported that the calcined mud decreased the autogenous shrinkage due to the formation of expansive calcium aluminate hydrates. Furthermore, they reported that SCC incorporating calcined mud showed denser microstructure and finer pore sizes, hence resulting in lower porosity, permeability, water diffusivity, and drying shrinkage. Zhang et al. [70] demonstrated that drying shrinkage is well correlated with pore volume, where lower volume of the mesopores below 50 nm can significantly decrease drying shrinkage. On the other hand, Collins and Sanjayan [71] showed that increasing the volume of mesopore is responsible for increasing the drying shrinkage. Overall, it appears that the differences were not significant between the mixtures.

4.4.4. External sulfate attack

The degradation of concrete due to external sulfate attack is primarily related to the expansion of gypsum ($C\bar{S}H$) and ettringite ($C_6A\bar{S}_3H_{32}$) formed by the reaction of unreacted C_3A, monosulfate, and portlandite (CH) with sodium sulfate (Na_2SO_4) or magnesium sulfate ($MgSO_4$). The expansion results obtained after 24 weeks of exposure are shown in Fig. 9. As can be observed, a rapid initial expansion was noted during the first month of testing. Then, the expansion rate stabilized until the

336 12^{th} week, where the expansion was limited to 0.022%. Another peak occurred at the 18^{th} week
337 until reaching 0.036% at the 24^{th} week in the case of SCC-2. SCC-1 and SCC-R mixtures showed
338 similar trend, while SCC-2 mixture showed higher expansion starting from the 4^{th} week of
339 exposure, even though it contains the lowest C_3A content due to higher substitution of cement by
340 TMS. This is probably due to the formation of ettringite following reaction of Na_2SO_4 and C_3A or
341 CH. Indeed, SEM observations revealed that SCC-2 exhibits a disordered structure with numerous
342 sulfate phases and large number of open pores [22]. Diverse CH crystals were observed in SCC-2,
343 including thin hexagonal and globular crystals indicating the presence of alite and belite. In addition
344 to SEM observations, XRD analyses showed that increasing the TMS content promoted the
345 formation of ettringite. The pozzolanic activity binds CH released during hydration of C_3S and C_2S,
346 hence leaving less available CH for reaction with sulphates and preventing the formation of gypsum
347 [72]. Another possible explanation may be the higher effective *w/b* ratio, which could decrease the
348 pH of the pore solution resulting in C-S-H instability and releasing of Ca^{2+} ions. At lower pH,
349 ettringite also become unstable and decompose to gypsum generating smaller expansion [73,74].
350 The higher expansion and mass gain of SCC-2 specimens could also be explained by its higher
351 porosity and sorptivity compared to those of SCC-R and SCC-1 mixtures, which provided an open
352 pathway for sulfate ions. In general, the use of 10% TMS did not have a negative effect on sulfate
353 attack.

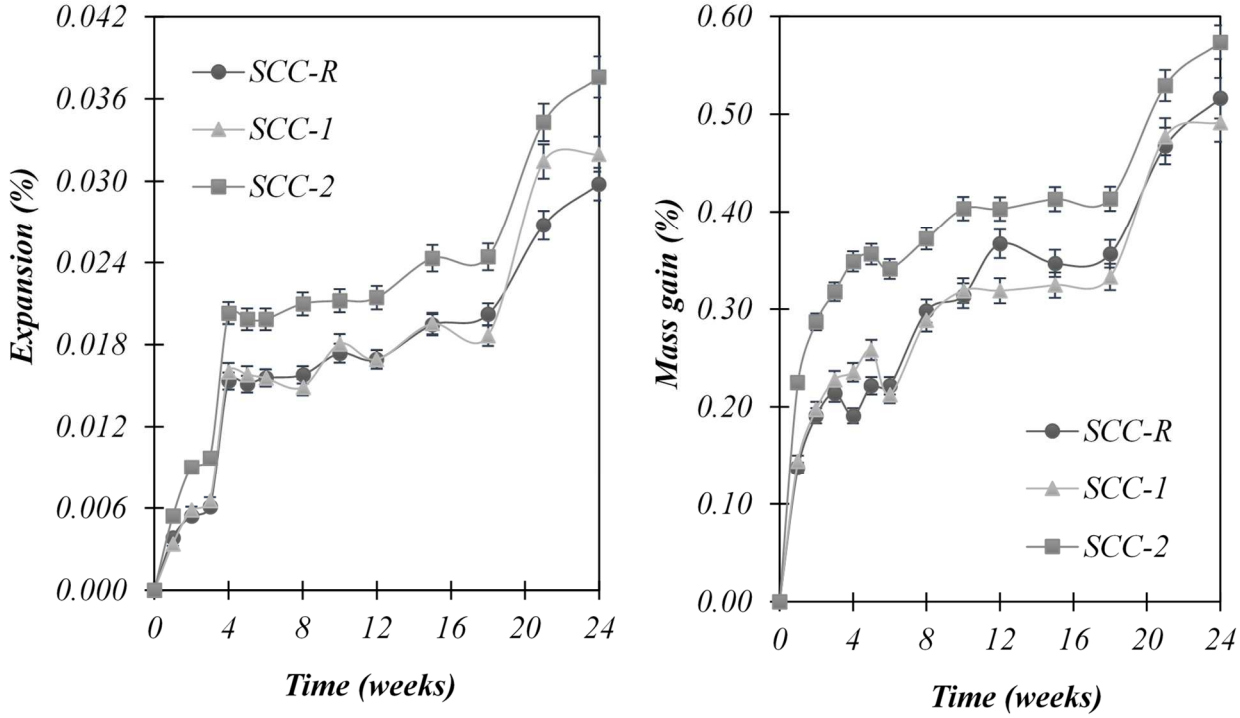

Fig. 9: Resistance to external sulfate attack: left) length expansion and right) mass gain

4.4.5. Accelerated Alkali Silica Testing

Mortar samples were prepared using a non-reactive sand and subjected to the accelerated alkali-silica test according to the ASTM C1260 specifications. The expansion and mass gain results are summarized in Fig. 10. As can be observed, a rapid expansion of 0.035% was observed after 3 days of exposure, regardless of the type of mixture. SCC-1 and SCC-R mixtures achieved comparable expansion of 0.070%, while SCC-2 exhibited slightly higher expansion of 0.075% after 14 days of exposure. On the other hand, the investigated mixtures exhibited almost the same mass gain where a slight increase of 1.0% was observed after 14 days of exposure. Overall, the expansions of the investigated mortar mixtures are lower than 0.10% after 14 days of exposure, hence reflecting an innocuous behavior according to the ASTM C1260 specifications [48]. These results indicate that the use of up to 20% TMS will not cause more ASR expansion under normal conditions, including the use of non-reactive aggregate.

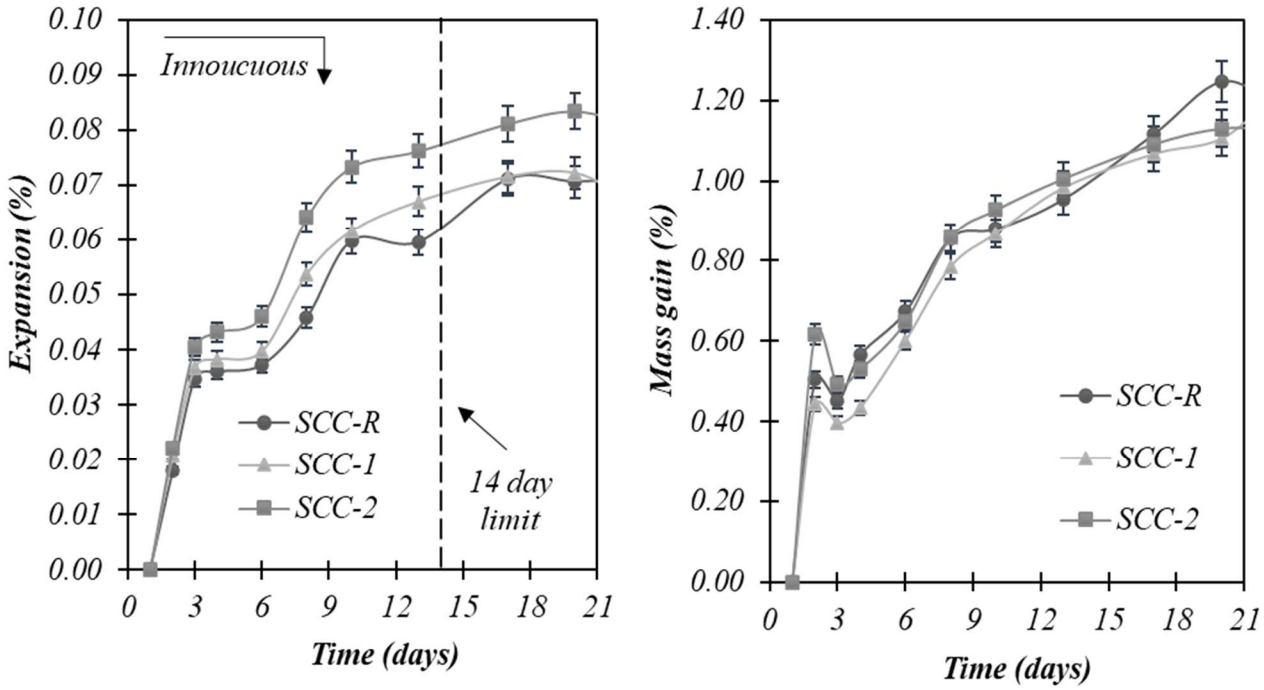

Fig. 10: Resistance to alkali silica reaction: left) expansion and right) weight gain

These results confirm the findings reported by Schwarz et al. [27] where expansion for mortars containing ternary mixture of cement, fly ash, and glass powder (5%, 10%, and 15%) showed an innocuous behavior less than 0.10%. Taha and Nounu [34] in their study on ASR testing of mortars containing 10% glass powder, they explained the findings by the quick dissolving of reactive silica during the pozzolanic reaction that agglomerated in the crystals of concrete minerals, hence may not be available for the ASR that occurs in later stages. They argue that in the first 4 weeks of pozzolanic reaction and hydration process, most of alkalis would have been consumed to catalyze the pozzolanic reaction and act as chemical activators to compensate for the lower calcium content in the glass powder.

4.4.6. Accelerated carbonation

Carbonation is one of the major factors affecting durability of concrete by reducing its pH, which can initiate the reinforcement corrosion. In fact, CO_2 in the air can react with hydration products, such as CH and C–S–H dissolved in pore water, to form $CaCO_3$ and water [75,76] according to the following equations:

$$Ca(OH)_2 + CO_2 \rightarrow CaCO_3 + H_2O \qquad \textit{Eq. 1}$$

$$(CaO)_x(SiO_2)_y(H_2O)_z + (x - x')CO_2 \rightarrow (CaO)_{x'}(SiO_2)_yH_{z'} + (\mathrm{x} - \mathrm{x}')CaCO_3 + (\mathrm{z} - \mathrm{z}')H_2O \qquad \textit{Eq. 2}$$

The carbonation of $Ca(OH)_2$ causes expansion, decreasing porosity, refining pores, increasing strength, and improving durability of the matrix [77]. However, carbonation of C–S–H cause its disintegration and loss of strength [78]. Assuming that carbonation process is steady, the depth (x_c) can be calculated using the Fick's first law as shown in Eq. 3.

$$x_C = k\sqrt{t} \qquad \textit{Eq. 3}$$

where k is the carbonation rate of concrete. The coefficient k_{acc}, which is related to the controlled test conditions, was determined for all the investigated SCC mixtures (Fig. 11). The test results revealed that the investigated mixtures showed seems to be proportional to the TMS replacement percentage. After 91 days of exposure, the carbonation depth of SCC-R reached 4 mm, while those of SCC-1 and SCC-2 reached 150% and 200% higher values, respectively. This can be due to the higher porosity and sorptivity of SCC mixtures containing TMS. As discussed earlier, increasing TMS content increases the effective *w/b* ratio, which results in lowering the pH of the matrix. Gabrisova et al. [79] conducted potentiometric analysis and concluded that ettringite is unstable below a pH of 10.7, while the monosulphate is unstable below 11.6; lowering the pH causes dissociation of phases, thus providing more calcium hydroxide (CH) available for carbonation. Matos and Sousa-Coutinho [59] reported similar carbonation trend, i.e. incorporating glass powder by 10% to 20% generates a carbonation depth of 5 mm and 8 mm, respectively, after 4 months of age. These values represent an increase of 165% and 265% compared to the reference, respectively.

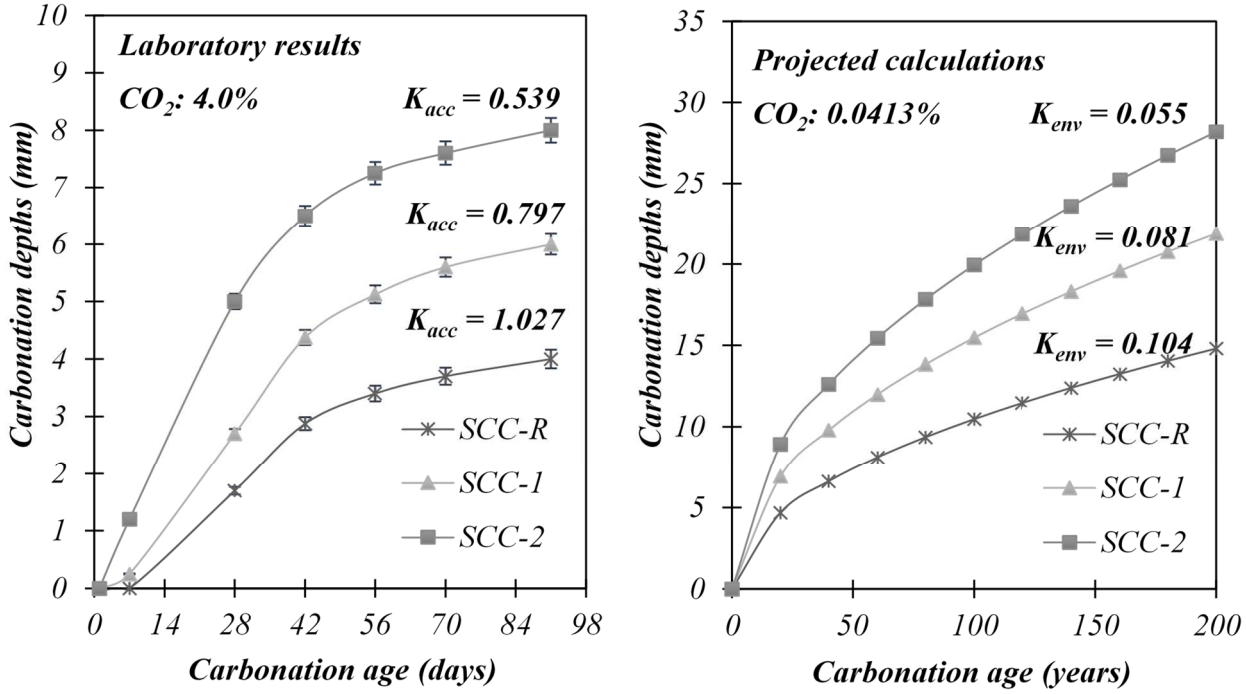

405

406 *Fig. 11 : Carbonation progress of the investigated SCC mixtures: left) in the tested atmosphere and*
407 *right) the consequential calculated development in air*

408 Sisomphon and Franke [80] proposed a relationship between k_{acc} and coefficient of environmental
409 carbonation (k_{env}), as follows:

410 $$k_{acc}/k_{env} = \sqrt{C_{acc}}/\sqrt{C_{env}} \qquad Eq.\ 4$$

411 where C_{acc} is the CO_2 concentration used to carry out the test (4.0%), while C_{env} is the CO_2
412 concentration in the environment, which varies from 0.03% in a rural environment to 0.1% in urban
413 areas [81]. According to NOAA Earth System Research Laboratory, the environment CO_2
414 concentration was fixed at 0.0413%. This scale up does not consider the influence of ambient
415 temperature and humidity, moisture cycles, and surface geometry, which could affect the
416 carbonation kinetics [24]. Using Eq. 3 and 4, the parameter k_{env} was calculated, and the carbonation
417 progression in nature was evaluated based on the √t-function (Fig. 11). For example, in the case of
418 20-mm concrete cover, the carbonation can reach the reinforcing bars after 167 and 101 years in the
419 case of SCC-1 and SCC-2 mixtures, respectively, compared to 365 years for the control mixture.

Even for the highest TMS content of 20%, the expected durability against carbonation is over 100 years.

4.5. Discussions

The high alkalinity of the pore solution rich in Ca^{2+}, SiO_4^{2-}, and OH^- ions contribute to dissolving the amorphous silica in TMS (Si–O–Si bond), which can react with Ca^{2+} ions to form C–S–H gel with a lower Ca/Si ratio. Higher substitution rates lead to a lower availability of Ca^{2+} to accommodate the higher existing Si brought by TMS, which can therefore delay cement hydration [35]. Less available Ca^{2+} can result in a decrease of pH of the pore solution, as reported by Du and Tan [73]. The pozzolanic reactivity of TMS depends on the substitution percentage and the mixture parameters, including the mixing water. Indeed, SCC-2 mixture proportioned with 20% TMS substitution showed slower strength development but reached equivalent mechanical properties after 90 days of age.

The curing type and duration, as well as temperature are key factors affecting the performance of SCM in terms of the strength development, especially in the case of rich-silica medium, such as that containing glass powder or TMS investigated in this study. Shi et al. [83] investigated the compressive strength of mortars made with glass powder and cured at different temperatures of 23°C, 35°C, and 65°C. As expected, mortar samples cured at 35°C and 65°C developed higher strength than those cured at 23°C, regardless of the age of mortar. This can be attributed to the higher apparent activation energy for pozzolanic reaction. Furthermore, Mirzahosseini and Riding [29] reported that mortar mixtures made with 25% glass powder and cured at 50 °C developed 25% higher compressive strength after 91 days than those cured at 23 °C. In the case of the investigated TMS, higher curing time can allow better mechanical performances.

The degradation mechanisms are related to the transport properties, including the sorptivity, which is a fundamental parameter controlling liquid transport in porous materials. Laidani et al. [84] investigated the effects of calcined bentonite on SCC properties and reported a strong

correlation between the chloride diffusion and porosity, and gas permeability and porosity. A low porosity was found to be associated with low passing charge and gas permeability coefficient. Kanellopoulos et al. [85] found a strong linear correlation ($R^2 = 0.94$) between sorptivity and open porosity, sorptivity and chloride permeability ($R^2 = 0.92$), as well as sorptivity and compressive strength ($R^2 = 0.93$). The authors [85] suggested that these durability properties are interrelated and constitute good indicators for durability. They can also be used to avoid long-term durability tests. Liu [57] also found a strong correlation between sorptivity and compressive strength ($R^2 = 0.82$) and suggested that sorptivity could be used to predict the service life of concrete.

A correlation was established between the total porosity and transport properties, including initial and final sorptivities, carbonation coefficient k_{acc}, and the chloride ions penetration. A strong correlation ($R^2 > 0.94$) between the total porosity and other transport properties was reported, as shown in Fig. 12 and Table 4. As expected, lower porosity was associated with lower sorptivity, carbonation permeability, and chloride diffusion. A high porosity was also related to a high diffusion of sulfate and NaOH used for ASR, where more expansion was observed in the case of SCC-2 due to its higher porous structure. Grinding TMS to meet a $d_{50} < 5$ µm can be interesting to ensure more reactive particles, hence resulting in denser and less porous ITZ.

Table 4: Transport properties of the investigated SCC mixtures

Mixes	***Total porosity (%)***	***Initial sorptivity ($mm^3/mm^2.s^{½}$)***	***Final sorptivity ($mm^3/mm^2.s^{½}$)***	***Chloride ions penetrability (C)***	***Carbonation k_{acc} (mm.day)***
SCC-R	8.74	2.81 E^{-3}	2.54 E^{-3}	341	0.539
SCC-1	9.08 (+3.9%)	3.02 E^{-3} (+7.5%)	3.48 E^{-3} (+37%)	354 (+3.8%)	0.797 (+50%)
SCC-2	9.57 (+9.5%)	3.37 E^{-3} (+20%)	4.11 E^{-3} (+62%)	406 (+19%)	1.027 (+90%)

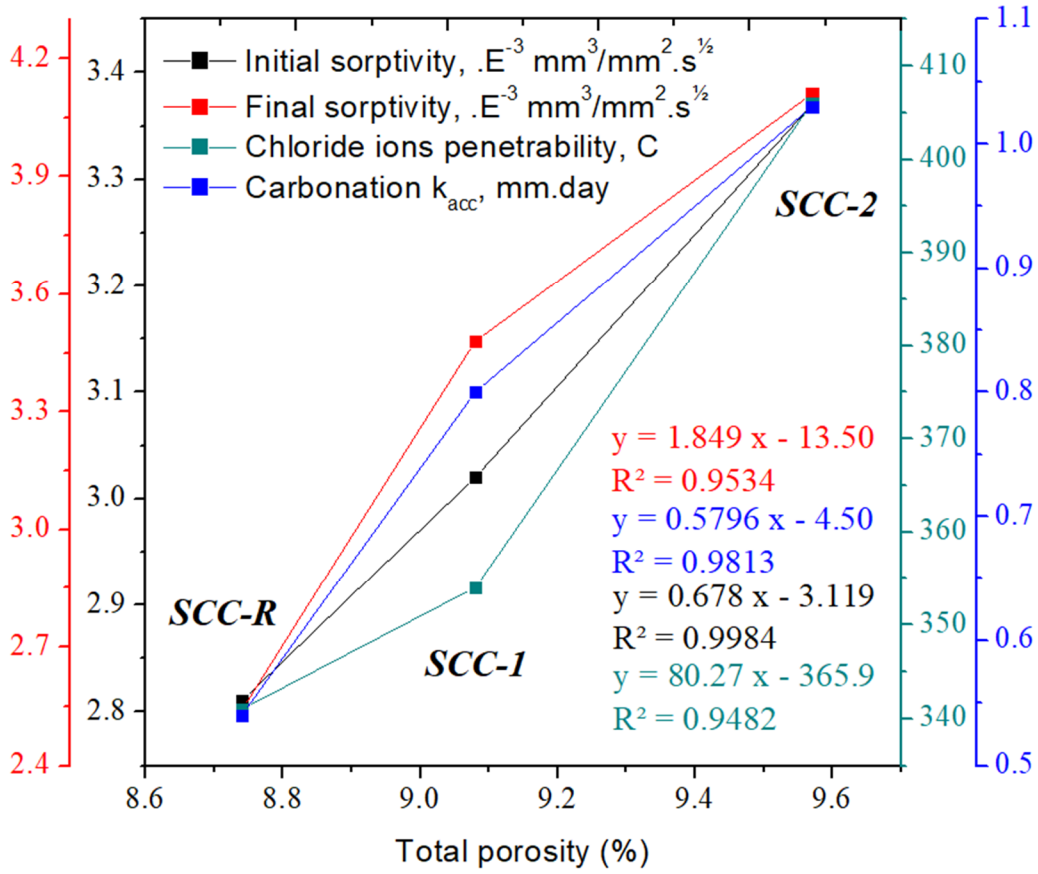

462

463 *Fig. 12: Correlation between various investigated transport properties*

464 The investigated SCCs met the criteria for high-performance SCC, including a fresh air content
465 of 5–8% [86] for durability purposes, high-early compression strength of 20–28 MPa, 28-d
466 compressive strength higher than 40 MPa (ASTM C39 [41]), low permeability of 500–2000
467 coulombs (ASTM C1202 [44]), low water absorption of 2–5%, expansion to sulfate attack below
468 0.10% after 6 months of exposure (ASTM C1012 [47]), high-elasticity modulus of 40 GPa (ASTM
469 C469 [87]), a drying shrinkage lower than 400 millionths (ASTM C157 [46]) [88], ultrasonic pulse
470 velocity higher than 4575 m/s [89], total porosity of 7–15% [90], and electrical resistance to
471 corrosion higher than 5–10 kΩ.cm [61].

472 ## 5. CONCLUSIONS

473 Key fresh and hardened properties, microstructure characterization, transport properties, and key
474 durability indicators of SCC containing treated marine sediments (TMS) were assessed. Based on
475 the results presented in this paper, the following conclusions can be pointed out:

1. The investigated SCC mixtures exhibited adequate self-consolidating characteristics with high filling and passing abilities, and good stability. Also, they exhibited comparable compressive splitting tensile strength values of 66 ± 1 MPa and 6 ± 0.3 MPa at 91 days, respectively.
2. An average total porosity of 9 ± 0.4% was found for the investigated mixtures. However, the incorporation of TMS increased the micropores volume (16%), decreased mesopores volume (44%), and decreased macropores volume (90%) compared to the reference mixture. This was attributed to the pozzolanic reaction and filling ability that refined the ITZ.
3. All the investigated SCC mixtures showed adequate transport property reflected by sorptivity values lower than 0.05 $mm^3/mm^2.s^{½}$. The incorporation of TMS increased the absorption and sorptivity by 7.5% and 19.8% in the case of SCC-1 and SCC-2 containing 10% and 20% TMS, respectively, compared to control mixture (2.81 E^{-3} $mm^3/mm^2.s^{½}$). In the case of the secondary sorptivity, higher increase of 37% (SCC-1) and 62% (SCC-2) were observed.
4. SCC mixture containing 10% TMS exhibited the highest electrical resistivity regardless of the age (8.1% higher than the reference of 470 kΩ.cm after 91 days). The use of higher TMS content resulted in higher chloride permeability by 19% compared to reference mixture (341 Coulombs).
5. SCC mixtures incorporating TMS exhibited lower drying shrinkage compared to the reference mixture. Control SCC mixture exhibited higher shrinkage after 49 days of exposure compared with those containing TMS.
6. For external sulfate attack, the use of 20% TMS led to a higher expansion compared with the reference mixture. The use of 10% TMS resulted in comparable expansion to that of the control mixture; however, the expansion was less than 10% after 24 weeks of exposure.
7. The use of TMS increased the carbonation depth compared to control mixture (4 mm) after 91 days of exposure by 150% (10% TMS) and 200% (20% TMS). The expected durability against carbonation of the investigated mixture is higher than 100 years.

8. Taken as a whole, incorporation up to 10% led to a comparable durability performance. A typical substitution rate of 10%-20% TMS can be considered without mitigating durability of non-reinforced concrete in moderate exposure class and no external aggression.

DECLARATIONS

Competing interest

We pledge that we are not involved in the interests of the financial, commercial, legal, or professional relationship with other organizations, or with the people we worked with them, that could influence this research.

Data availability

The data supporting the conclusions of this article are included within the article. Any queries regarding these data may be directed to the corresponding author.

Funding

The research work was accomplished as a part of a PhD program [91] in the laboratory of the *Department of Civil & Building Engineering* of the *Université de Sherbrooke*, Canada. The study was funded by the research funds of the *IMT Lille Douai*, grants from the *Natural Sciences and Engineering Research Council of Canada* (NSERC) and the "*Fonds de Recherche Nature et Technologies du Québec*" (FRQNT). A. M. Safhi thanks the *ACI-Quebec and East Ontario Chapter* for supporting this work through "Michel Pigeon" award. The authors would like to thank Sika Canada, Montreal, for providing the admixtures.

REFERENCES

[1] CEN/TC 104 "Concrete and related products" technical committee., EN 206+A1 : Concrete – Part 1: Specification, performance, production and conformity, (2016).

[2] J.G. Kessy, M.G. Alexander, H. Beushausen, Concrete durability standards: International trends and the South African context, J. South Afr. Inst. Civ. Eng. 57 (2015) 47–58. https://doi.org/10.17159/2309-8775/2015/v57n1a5.

[3] M. Cyr, 8 - Influence of supplementary cementitious materials (SCMs) on concrete durability, in: Eco-Effic. Concr., Woodhead Publishing, 2013: pp. 153–197. https://doi.org/10.1533/9780857098993.2.153.

[4] J.M. Marangu, J.K. Thiong'o, J.M. Wachira, Chloride Ingress in Chemically Activated Calcined Clay-Based Cement, J. Chem. 2018 (2018) e1595230. https://doi.org/10.1155/2018/1595230.

[5] J.M. Marangu, J.K. Thiong'o, J.M. Wachira, Review of Carbonation Resistance in Hydrated Cement Based Materials, J. Chem. 2019 (2019) e8489671. https://doi.org/10.1155/2019/8489671.

[6] A.S. El-Dieb, D.M. Kanaan, Ceramic waste powder an alternative cement replacement – Characterization and evaluation, Sustain. Mater. Technol. 17 (2018) e00063. https://doi.org/10.1016/j.susmat.2018.e00063.

[7] M. Abed, R. Nemes, Long-term durability of self-compacting high-performance concrete produced with waste materials, Constr. Build. Mater. 212 (2019) 350–361. https://doi.org/10.1016/j.conbuildmat.2019.04.004.

[8] Z. Ahmadi, J. Esmaeili, J. Kasaei, R. Hajialioghli, Properties of sustainable cement mortars containing high volume of raw diatomite, Sustain. Mater. Technol. 16 (2018) 47–53. https://doi.org/10.1016/j.susmat.2018.05.001.

[9] F.A. Sabet, N.A. Libre, M. Shekarchi, Mechanical and durability properties of self consolidating high performance concrete incorporating natural zeolite, silica fume and fly ash, Constr. Build. Mater. 44 (2013) 175–184. https://doi.org/10.1016/j.conbuildmat.2013.02.069.

547 [10] P. Hou, S. Kawashima, D. Kong, D.J. Corr, J. Qian, S.P. Shah, Modification effects of
548 colloidal nanoSiO2 on cement hydration and its gel property, Compos. Part B Eng. 45 (2013)
549 440–448. https://doi.org/10.1016/j.compositesb.2012.05.056.
550 [11] D. Kong, Y. Su, X. Du, Y. Yang, S. Wei, S.P. Shah, Influence of nano-silica agglomeration on
551 fresh properties of cement pastes, Constr. Build. Mater. 43 (2013) 557–562.
552 https://doi.org/10.1016/j.conbuildmat.2013.02.066.
553 [12] K. Jaglal, D.M. Crawford, S.W. Anagnost, B.E. White, Alternative Approaches for Managing
554 Dredged Sediments, in: Proceeding of the Western Dredging Association (WEDA),
555 Vancouver, British Columbia, Canada, 2017.
556 [13] J. Harrington, J. Murphy, M. Coleman, D. Jordan, T. Debuigne, G. Szacsuri, Economic
557 modelling of the management of dredged marine sediments, Geol. Geophys. Environ. 42
558 (2016) 311. https://doi.org/10.7494/geol.2016.42.3.311.
559 [14] M. Benzerzour, M. Amar, N.-E. Abriak, New experimental approach of the reuse of dredged
560 sediments in a cement matrix by physical and heat treatment, Constr. Build. Mater. 140 (2017)
561 432–444. https://doi.org/10.1016/j.conbuildmat.2017.02.142.
562 [15] M. Amar, M. Benzerzour, N.-E. Abriak, Y. Mamindy-Pajany, Study of the pozzolanic activity
563 of a dredged sediment from Dunkirk harbour, Powder Technol. 320 (2017) 748–764.
564 https://doi.org/10.1016/j.powtec.2017.07.055.
565 [16] R. Snellings, Ö. Cizer, L. Horckmans, P.T. Durdziński, P. Dierckx, P. Nielsen, K. Van Balen,
566 L. Vandewalle, Properties and pozzolanic reactivity of flash calcined dredging sediments,
567 Appl. Clay Sci. 129 (2016) 35–39. https://doi.org/10.1016/j.clay.2016.04.019.
568 [17] F. Rozas, A. Castillo, I. Martínez, M. Castellote, Guidelines for assessing the valorization of a
569 waste into cementitious material: dredged sediment for production of self compacting
570 concrete, Mater. Constr. 65 (2015) 057. https://doi.org/10.3989/mc.2015.10613.

571 [18] E. Rozière, M. Samara, A. Loukili, D. Damidot, Valorisation of sediments in self-
572 consolidating concrete: Mix-design and microstructure, Constr. Build. Mater. 81 (2015) 1–10.
573 https://doi.org/10.1016/j.conbuildmat.2015.01.080.
574 [19] N.-E. Bouhamou, F. Mostefa, A. Mebrouki, K. Bendani, N. Belas, Influence of dredged
575 sediment on the shrinkage behavior of self-compacting concrete, Mater. Tehnol. 50 (2016)
576 127–135. https://doi.org/10.17222/mit.2013.252.
577 [20] A. el M. Safhi, M. Benzerzour, P. Rivard, N.-E. Abriak, Feasibility of using marine sediments
578 in SCC pastes as supplementary cementitious materials, Powder Technol. (2018).
579 https://doi.org/10.1016/j.powtec.2018.12.060.
580 [21] A. el M. Safhi, M. Benzerzour, P. Rivard, N.-E. Abriak, I. Ennahal, Development of self-
581 compacting mortars based on treated marine sediments, J. Build. Eng. 22 (2019) 252–261.
582 https://doi.org/10.1016/j.jobe.2018.12.024.
583 [22] A. el M. Safhi, P. Rivard, A. Yahia, M. Benzerzour, K.H. Khayat, Valorization of dredged
584 sediments in self-consolidating concrete: Fresh, hardened, and microstructural properties, J.
585 Clean. Prod. 263 (2020) 121472. https://doi.org/10.1016/j.jclepro.2020.121472.
586 [23] ASTM C150, Specification for Portland Cement, ASTM International, 2019.
587 https://doi.org/10.1520/C0150_C0150M-19A.
588 [24] ASTM C618, Specification for Coal Fly Ash and Raw or Calcined Natural Pozzolan for Use in
589 Concrete, ASTM International, 2019. https://doi.org/10.1520/C0618-19.
590 [25] Y. Sharifi, I. Afshoon, Z. Firoozjaei, A. Momeni, Utilization of Waste Glass Micro-particles in
591 Producing Self-Consolidating Concrete Mixtures, Int. J. Concr. Struct. Mater. 10 (2016) 337.
592 https://doi.org/10.1007/s40069-016-0141-z.
593 [26] H. Du, K.H. Tan, Properties of high volume glass powder concrete, Cem. Concr. Compos. 75
594 (2017) 22–29. https://doi.org/10.1016/j.cemconcomp.2016.10.010.

595 [27] N. Schwarz, N. Neithalath, Influence of a fine glass powder on cement hydration: Comparison
596 to fly ash and modeling the degree of hydration, Cem. Concr. Res. 38 (2008) 429–436.
597 https://doi.org/10.1016/j.cemconres.2007.12.001.
598 [28] Y. Shao, T. Lefort, S. Moras, D. Rodriguez, Studies on concrete containing ground waste
599 glass, Cem. Concr. Res. 30 (2000) 91–100. https://doi.org/10.1016/S0008-8846(99)00213-6.
600 [29] M. Mirzahosseini, K.A. Riding, Effect of curing temperature and glass type on the pozzolanic
601 reactivity of glass powder, Cem. Concr. Res. 58 (2014) 103–111.
602 https://doi.org/10.1016/j.cemconres.2014.01.015.
603 [30] M.C. Bignozzi, A. Saccani, L. Barbieri, I. Lancellotti, Glass waste as supplementary
604 cementing materials: The effects of glass chemical composition, Cem. Concr. Compos. 55
605 (2015) 45–52. https://doi.org/10.1016/j.cemconcomp.2014.07.020.
606 [31] H. Lee, A. Hanif, M. Usman, J. Sim, H. Oh, Performance evaluation of concrete incorporating
607 glass powder and glass sludge wastes as supplementary cementing material, J. Clean. Prod.
608 170 (2018) 683–693. https://doi.org/10.1016/j.jclepro.2017.09.133.
609 [32] J. Lu, Z. Duan, C.S. Poon, Combined use of waste glass powder and cullet in architectural
610 mortar, Cem. Concr. Compos. 82 (2017) 34–44.
611 https://doi.org/10.1016/j.cemconcomp.2017.05.011.
612 [33] A. Bouchikhi, M. Benzerzour, N.-E. Abriak, W. Maherzi, Y. Mamindy-Pajany, Study of the
613 impact of waste glasses types on pozzolanic activity of cementitious matrix, Constr. Build.
614 Mater. 197 (2019) 626–640. https://doi.org/10.1016/j.conbuildmat.2018.11.180.
615 [34] B. Taha, G. Nounu, Properties of concrete contains mixed colour waste recycled glass as sand
616 and cement replacement, Constr. Build. Mater. 22 (2008) 713–720.
617 https://doi.org/10.1016/j.conbuildmat.2007.01.019.
618 [35] B. Lothenbach, K. Scrivener, R.D. Hooton, Supplementary cementitious materials, Cem.
619 Concr. Res. 41 (2011) 1244–1256. https://doi.org/10.1016/j.cemconres.2010.12.001.

620 [36] D.R. Gaskell, CHAPTER FOURTEEN - THE DETERMINATION OF PHASE DIAGRAMS
621 FOR SLAG SYSTEMS, in: J.-C. Zhao (Ed.), Methods Phase Diagr. Determ., Elsevier Science
622 Ltd, Oxford, 2007: pp. 442–458. https://doi.org/10.1016/B978-008044629-5/50014-8.
623 [37] T. Sedran, F.D. Larrard, L.L. Guen, Détermination de la compacité des ciments et additions
624 minérales à la sonde de Vicat, Bull. Lab. Ponts Chaussées. (2007) 155–163.
625 [38] ASTM C1611, Test Method for Slump Flow of Self-Consolidating Concrete, ASTM
626 International, 2019. https://doi.org/10.1520/C1611_C1611M-18.
627 [39] ASTM C1621, Test Method for Passing Ability of Self-Consolidating Concrete by J-Ring,
628 ASTM International, 2017. https://doi.org/10.1520/C1621_C1621M-17.
629 [40] ASTM C231, Test Method for Air Content of Freshly Mixed Concrete by the Pressure
630 Method, ASTM International, 2017. https://doi.org/10.1520/C0231_C0231M-17A.
631 [41] ASTM C39, Test Method for Compressive Strength of Cylindrical Concrete Specimens,
632 ASTM International, 2018. https://doi.org/10.1520/C0039_C0039M-18.
633 [42] ASTM C496, Test Method for Splitting Tensile Strength of Cylindrical Concrete Specimens,
634 ASTM International, 2017. https://doi.org/10.1520/C0496_C0496M-17.
635 [43] ASTM C1760, Test Method for Bulk Electrical Conductivity of Hardened Concrete, ASTM
636 International, 2012. https://doi.org/10.1520/C1760-12.
637 [44] ASTM C1202, Test Method for Electrical Indication of Concretes Ability to Resist Chloride
638 Ion Penetration, ASTM International, 2019. https://doi.org/10.1520/C1202-19.
639 [45] ASTM C1582, Specification for Admixtures to Inhibit Chloride-Induced Corrosion of
640 Reinforcing Steel in Concrete, ASTM International, 2017.
641 https://doi.org/10.1520/C1582_C1582M-11R17E01.
642 [46] ASTM C157, Test Method for Length Change of Hardened Hydraulic-Cement Mortar and
643 Concrete, ASTM International, 2017. https://doi.org/10.1520/C0157_C0157M-17.
644 [47] ASTM C1012, Test Method for Length Change of Hydraulic-Cement Mortars Exposed to a
645 Sulfate Solution, ASTM International, 2018. https://doi.org/10.1520/C1012_C1012M-18B.

646 [48] ASTM C1260, Test Method for Potential Alkali Reactivity of Aggregates (Mortar-Bar
647 Method), ASTM International, 2014. https://doi.org/10.1520/C1260-14.
648 [49] Self-Compacting Concrete European Project Group, The European Guidelines for Self-
649 compacting Concrete: Specification, Production and Use, International Bureau for Precast
650 Concrete (BIBM), 2005.
651 [50] ACI Committee 237, ed., Self-consolidating concrete, American Concrete Institute,
652 Farmington Hills, Mich, 2007.
653 [51] K.H. Khayat, J. Assaad, J. Daczko, Comparison of Field-Oriented Test Methods to Assess
654 Dynamic Stability of Self-Consolidating Concrete, ACI Mater. J. 101 (2004).
655 https://doi.org/10.14359/13066.
656 [52] B.V. Kavyateja, J. Guru Jawahar, C. Sashidhar, Effectiveness of alccofine and fly ash on
657 mechanical properties of ternary blended self compacting concrete, Mater. Today Proc.
658 (2020). https://doi.org/10.1016/j.matpr.2020.03.152.
659 [53] P. Duan, Z. Shui, W. Chen, C. Shen, Effects of metakaolin, silica fume and slag on pore
660 structure, interfacial transition zone and compressive strength of concrete, Constr. Build.
661 Mater. 44 (2013) 1–6. https://doi.org/10.1016/j.conbuildmat.2013.02.075.
662 [54] Q. Zeng, K. Li, T. Fen-Chong, P. Dangla, Analysis of pore structure, contact angle and pore
663 entrapment of blended cement pastes from mercury porosimetry data, Cem. Concr. Compos.
664 34 (2012) 1053–1060. https://doi.org/10.1016/j.cemconcomp.2012.06.005.
665 [55] N.S. Martys, C.F. Ferraris, Capillary transport in mortars and concrete, Cem. Concr. Res. 27
666 (1997) 747–760. https://doi.org/10.1016/S0008-8846(97)00052-5.
667 [56] C. Hall, Water sorptivity of mortars and concretes: a review, Mag. Concr. Res. 41 (1989) 51–
668 61. https://doi.org/10.1680/macr.1989.41.147.51.
669 [57] M. Liu, Incorporating ground glass in self-compacting concrete, Constr. Build. Mater. 25
670 (2011) 919–925. https://doi.org/10.1016/j.conbuildmat.2010.06.092.

671 [58] R.-U.-D. Nassar, P. Soroushian, Strength and durability of recycled aggregate concrete
672 containing milled glass as partial replacement for cement, Constr. Build. Mater. 29 (2012)
673 368–377. https://doi.org/10.1016/j.conbuildmat.2011.10.061.
674 [59] A.M. Matos, J. Sousa-Coutinho, Durability of mortar using waste glass powder as cement
675 replacement, Constr. Build. Mater. 36 (2012) 205–215.
676 https://doi.org/10.1016/j.conbuildmat.2012.04.027.
677 [60] K.O. Ampadu, K. Torii, Chloride ingress and steel corrosion in cement mortars incorporating
678 low-quality fly ashes, Cem. Concr. Res. 32 (2002) 893–901. https://doi.org/10.1016/S0008-
679 8846(02)00721-4.
680 [61] Md. Safiuddin, J.S. West, K.A. Soudki, Hardened properties of self-consolidating high
681 performance concrete including rice husk ash, Cem. Concr. Compos. 32 (2010) 708–717.
682 https://doi.org/10.1016/j.cemconcomp.2010.07.006.
683 [62] M. Thomas, Specifying and Achieving Durable Concrete, in: Concr. NZ Conf. 2018 Tech.
684 Pap. TR71, Claudelands, Hamilton, 2018.
685 [63] H.S. Al-alaily, A.A.A. Hassan, Time-dependence of chloride diffusion for concrete containing
686 metakaolin, J. Build. Eng. 7 (2016) 159–169. https://doi.org/10.1016/j.jobe.2016.06.003.
687 [64] Y. Dhandapani, T. Sakthivel, M. Santhanam, R. Gettu, R.G. Pillai, Mechanical properties and
688 durability performance of concretes with Limestone Calcined Clay Cement (LC3), Cem.
689 Concr. Res. 107 (2018) 136–151. https://doi.org/10.1016/j.cemconres.2018.02.005.
690 [65] M. Alexander, M. Thomas, Service life prediction and performance testing — Current
691 developments and practical applications, Cem. Concr. Res. 78 (2015) 155–164.
692 https://doi.org/10.1016/j.cemconres.2015.05.013.
693 [66] A.A. Abouhussien, A.A.A. Hassan, Optimizing the durability and service life of self-
694 consolidating concrete containing metakaolin using statistical analysis, Constr. Build. Mater.
695 76 (2015) 297–306. https://doi.org/10.1016/j.conbuildmat.2014.12.010.

[67] K. Obla, C. Lobo, H. Kim, Tests and Criteria for Concrete Resistant to Chloride Ion Penetration, ACI Mater. J. 113 (2016). https://doi.org/10.14359/51689107.

[68] A.A. Ramezanianpour, H. Bahrami Jovein, Influence of metakaolin as supplementary cementing material on strength and durability of concretes, Constr. Build. Mater. 30 (2012) 470–479. https://doi.org/10.1016/j.conbuildmat.2011.12.050.

[69] R.-X. Liu, C.-S. Poon, Utilization of red mud derived from bauxite in self-compacting concrete, J. Clean. Prod. 112 (2016) 384–391. https://doi.org/10.1016/j.jclepro.2015.09.049.

[70] W. Zhang, Y. Hama, S.H. Na, Drying shrinkage and microstructure characteristics of mortar incorporating ground granulated blast furnace slag and shrinkage reducing admixture, Constr. Build. Mater. 93 (2015) 267–277. https://doi.org/10.1016/j.conbuildmat.2015.05.103.

[71] F. Collins, J.G. Sanjayan, Effect of pore size distribution on drying shrinking of alkali-activated slag concrete, Cem. Concr. Res. 30 (2000) 1401–1406. https://doi.org/10.1016/S0008-8846(00)00327-6.

[72] M. Sahmaran, O. Kasap, K. Duru, I.O. Yaman, Effects of mix composition and water–cement ratio on the sulfate resistance of blended cements, Cem. Concr. Compos. 29 (2007) 159–167. https://doi.org/10.1016/j.cemconcomp.2006.11.007.

[73] H. Du, K.H. Tan, Transport Properties of Concrete with Glass Powder as Supplementary Cementitious Material, ACI Mater. J. 112 (2015). https://doi.org/10.14359/51687363.

[74] D.J. De Souza, M.H.F. Medeiros, J. Hoppe, L.F.M. Sanchez, The Uses of Finely Ground Materials to Mitigate the External Sulphate Attack (ESA) on Cementitious Materials, in: E. Menéndez, V. Baroghel-Bouny (Eds.), Extern. Sulphate Attack – Field Asp. Lab Tests, Springer International Publishing, Cham, 2020: pp. 139–151. https://doi.org/10.1007/978-3-030-20331-3_11.

[75] W.-J. Long, Y. Gu, F. Xing, K.H. Khayat, Microstructure development and mechanism of hardened cement paste incorporating graphene oxide during carbonation, Cem. Concr. Compos. 94 (2018) 72–84. https://doi.org/10.1016/j.cemconcomp.2018.08.016.

722 [76] M. Boumaaza, B. Huet, P. Turcry, A. Aït-Mokhtar, The CO2-binding capacity of synthetic
723 anhydrous and hydrates: Validation of a test method based on the instantaneous reaction rate,
724 Cem. Concr. Res. 135 (2020) 106113. https://doi.org/10.1016/j.cemconres.2020.106113.
725 [77] E.A.B. Khalil, M. Anwar, Carbonation of ternary cementitious concrete systems containing fly
726 ash and silica fume, Water Sci. 29 (2015) 36–44. https://doi.org/10.1016/j.wsj.2014.12.001.
727 [78] B. Lu, C. Shi, J. Zhang, J. Wang, Effects of carbonated hardened cement paste powder on
728 hydration and microstructure of Portland cement, Constr. Build. Mater. 186 (2018) 699–708.
729 https://doi.org/10.1016/j.conbuildmat.2018.07.159.
730 [79] A. Gabrisová, J. Havlica, S. Sahu, Stability of calcium sulphoaluminate hydrates in water
731 solutions with various pH values, Cem. Concr. Res. 21 (1991) 1023–1027.
732 https://doi.org/10.1016/0008-8846(91)90062-M.
733 [80] K. Sisomphon, L. Franke, Carbonation rates of concretes containing high volume of
734 pozzolanic materials, Cem. Concr. Res. 37 (2007) 1647–1653.
735 https://doi.org/10.1016/j.cemconres.2007.08.014.
736 [81] A.M. Neville, Properties of Concrete, 5 edition, Prentice Hall, Harlow, England ; New York,
737 2012.
738 [82] Chen Chun-Tao, Ho Chia-Wei, Influence of Cyclic Humidity on Carbonation of Concrete, J.
739 Mater. Civ. Eng. 25 (2013) 1929–1935. https://doi.org/10.1061/(ASCE)MT.1943-
740 5533.0000750.
741 [83] C. Shi, Y. Wu, C. Riefler, H. Wang, Characteristics and pozzolanic reactivity of glass
742 powders, Cem. Concr. Res. 35 (2005) 987–993.
743 https://doi.org/10.1016/j.cemconres.2004.05.015.
744 [84] Z.E.-A. Laidani, B. Benabed, R. Abousnina, M.K. Gueddouda, E.-H. Kadri, Experimental
745 investigation on effects of calcined bentonite on fresh, strength and durability properties of
746 sustainable self-compacting concrete, Constr. Build. Mater. 230 (2020) 117062.
747 https://doi.org/10.1016/j.conbuildmat.2019.117062.

748 [85] A. Kanellopoulos, M.F. Petrou, I. Ioannou, Durability performance of self-compacting
749 concrete, Constr. Build. Mater. 37 (2012) 320–325.
750 https://doi.org/10.1016/j.conbuildmat.2012.07.049.
751 [86] K.H. Khayat, Optimization and performance of air-entrained, self-consolidating concrete, ACI
752 Struct. J. 97 (2000) 526–535.
753 [87] ASTM C469, Test Method for Static Modulus of Elasticity and Poissons Ratio of Concrete in
754 Compression, ASTM International, 2014. https://doi.org/10.1520/C0469_C0469M-14.
755 [88] S.H. Kosmatka, B. Kerkhoff, W.C. Panarese, Design and control of concrete mixtures,
756 Portland Cement Association, Skokie, 2002.
757 [89] M.S. Shetty, Concrete technology: theory and practice, S. Chand, Ram Nagar, New Delhi,
758 2007.
759 [90] N. Hearn, R.D. Hooton, R.H. Mills, Pore Structure and Permeability, Significance Tests Prop.
760 Concr. Concr.-Mak. Mater. (1994). https://doi.org/10.1520/STP36424S.
761 [91] A. el M. SAFHI, Valorisation des sédiments de dragage dans des bétons autoplaçants :
762 optimisation de la formulation et étude de la durabilité, Recycling of dredged sediments in
763 self-consolidating concrete: mix design optimization and durability study. (2020).
764 http://hdl.handle.net/11143/16937.
765